

# Demonstration of a multiview projection display using decentered microlens arrays

Lawrence Bogaert,<sup>1,\*</sup> Yuri Meuret,<sup>1</sup> Stijn Roelandt,<sup>1</sup> Aykut Avci,<sup>2</sup>  
Herbert De Smet,<sup>2,3</sup> and Hugo Thienpont<sup>1</sup>

<sup>1</sup>Brussels Photonics Team, Vrije Universiteit Brussel, Pleinlaan 2, B-1050 Brussels, Belgium

<sup>2</sup>Electronics and Information Systems Department, Ghent University,  
Technologiepark 914, B-9052 Ghent, Belgium

<sup>3</sup>Centre for Microsystems Technology, imec, Technologiepark 914, B-9052 Ghent, Belgium

[lbogaert@b-phot.org](mailto:lbogaert@b-phot.org)

**Abstract:** In this work we present a prototype multiview projection display that combines high-spatial and high-angular resolution with low complexity, compact form factor and potentially low-cost design. The system consists of a single projector and an image steering projection screen. It is based on beam steering using decentered microlens arrays in the projection screen and time-sequential rear-projection of the view images. The prototype has a 25 in. screen, a total of 27 viewing zones with XGA resolution and a horizontal field of view of 30°.

© 2010 Optical Society of America

**OCIS codes:** (110.0110) Imaging systems, (120.2040) Displays, (100.6890) Three-dimensional image processing, (220.0220) Optical design and fabrication, (350.3950) Micro-optics.

---

## References and links

1. J. Son and B. Javidi, "Three-dimensional imaging methods based on multiview images," *J. Disp. Technol.* **1**, 125–140 (2005).
2. L. Lipton, "Digital stereoscopic cinema: the 21st century," in *Stereoscopic Displays and Applications XIX*, A. Woods, N. Holliman, and J. Merritt, eds., Proc. SPIE-IS&T Electronic Imaging **6803**, 68030W (2008).
3. Y. Kajiki, H. Yoshikawa, and T. Honda, "Hologram-like video images by 45-view stereoscopic display," in *Stereoscopic Displays and Virtual Reality Systems IV*, S. Fisher, J. Merritt, and M. Bolas, eds., Proc. SPIE **3012**, 154–166 (1997).
4. T. Honda and M. Shimomatsu, "Natural 3-D display system by a fan-like array of projection optics," in *Three-Dimensional TV, Video, and Display*, B. Javidi and F. Okano, eds., Proc. SPIE **4864**, 96–103 (2002).
5. Y. Takaki, "High-density directional display for generating natural three-dimensional images," *Proc. IEEE* **94**, 654–663 (2006).
6. O. Willemsen, S. de Zwart, M. Hiddink, D. de Boer, and M. Krijn, "Multi-view 3D displays," *SID Symposium Digest* **38**, 1154–1157 (2007).
7. M. Krijn, S. de Zwart, D. de Boer, O. Willemsen, and M. Sluijter, "2-D/3-D displays based on switchable lenticulars," *J. Soc. Inf. Display* **16**, 847–855 (2008).
8. B. Lee, H. Hong, J. Park, H. Park, H. Shin, and I. Jung, "Multiview autostereoscopic display of 36view using an ultra-high resolution LCD," in *Stereoscopic Displays and Virtual Reality Systems XIV*, A. Woods, N. Dodgson, J. Merritt, M. Bolas, and I. McDowall, eds., Proc. SPIE-IS&T Electronic Imaging **6490**, 64900S (2007).
9. Y. Takaki, O. Yokoyama, and G. Hamagishi, "Flat panel display with slanted pixel arrangement for 16-view display," in *Stereoscopic Displays and Applications XX*, A. Woods, N. Holliman, and J. Merritt, eds., Proc. SPIE-IS&T Electronic Imaging **7237**, 723708 (2009).
10. J. Son, V. Komar, Y. Chun, S. Sabo, V. Mayorov, L. Balasny, S. Belyaev, M. Semin, M. Krutik, and H. Jeon, "A multiview 3-D imaging system with full color capabilities," in *Stereoscopic Displays and Virtual Reality Systems V*, M. Bolas, S. Fisher, and J. Merritt, eds., Proc. SPIE **3295**, 218–223 (1998).

11. T. Kanebako and Y. Takaki, "Time-multiplexing display module for high-density directional display," in *Stereoscopic Displays and Applications XIX*, A. Woods, N. Holliman, and J. Merritt, eds., Proc. SPIE-IS&T Electronic Imaging **6803**, 68030P (2008).
12. L. Hornbeck, "Digital light processing for high-brightness high-resolution applications," in *Projection Displays III*, M. Wu, ed., Proc. SPIE **3013**, 27–40 (1997).
13. T. Balogh, "The HoloVizio system," in *Stereoscopic Displays and Virtual Reality Systems XIII*, A. Woods, N. Dodgson, J. Merritt, M. Bolas, and I. McDowall, eds., Proc. SPIE-IS&T Electronic Imaging **6055**, 60550U (2006).
14. K. Kikuta and Y. Takaki, "Development of SVGA resolution 128-directional display," in *Stereoscopic Displays and Virtual Reality Systems XIV*, A. Woods, N. Dodgson, J. Merritt, M. Bolas, and I. McDowall, eds., Proc. SPIE-IS&T Electronic Imaging **6490**, 64900U (2007).
15. Y. Takaki and N. Nago, "Multi-projection of lenticular displays to construct a 256-view super multi-view display," *Opt. Express* **18**, 8824–8835 (2010).
16. E. Watson, "Analysis of beam steering with decentered microlens arrays," *Opt. Eng.* **32**, 2665–2670 (1993).
17. J. Duparré, D. Radtke, and P. Dannberg, "Implementation of field lens arrays in beam-deflecting microlens array telescopes," *Appl. Opt.* **43**, 4854–4861 (2004).
18. J. Jang and B. Javidi, "Improved viewing resolution of three-dimensional integral imaging by use of nonstationary micro-optics," *Opt. Letters* **27**, 324–326 (2002).
19. W. Bleha and R. Sterling, "D-ILA technology for high resolution projection displays," in *Cockpit Displays X*, D. Hopper, ed., Proc. SPIE **5080**, 239–249 (2003).
20. S. Hashimoto, O. Akimoto, H. Ishikawa, T. Kiyomiya, T. Togawa, T. Isozaki, H. Abe, M. Nakai, H. Terakawa, H. Horikiri, T. Ishii, and M. Kogure, "SXRD (Silicon X-ray Reflective Display); a new display device for projection displays," *SID Symposium Digest* **36**, 1362–1365 (2005).
21. E. Wolterink and K. Demeyer, "Wafer optics mass volume production and reliability," in *Micro-Optics 2010*, H. Thienpont, P. V. Daele, J. Mohr, and H. Zappe, eds., Proc. SPIE **7716**, 771614 (2010).
22. Y. Cheng, F. Tsai, A. Wang, and H. Chiu, "High brightness LED based projector with NTSC 120% wide color gamut," *SID Symposium Digest* **41**, 976–978 (2010).
23. F. Fournier and J. Rolland, "Design methodology for high brightness projectors," *J. Disp. Technol.* **4**, 86–91 (2008).
24. E. Geißler, "Meeting the challenges of developing LED-based projection displays," in *Photonics in Multimedia*, A. Tervonen, M. Kujawinska, W. IJzerman, and H. De Smet, eds., Proc. SPIE **6196**, 619601 (2006).
25. S. Roelandt, L. Bogaert, Y. Meuret, A. Avcı, H. De Smet, and H. Thienpont, "Color uniformity in compact LED illumination for DMD projectors," in *Optics, Photonics, and Digital Technologies for Multimedia Applications*, P. Schelkens, T. Ebrahimi, G. Cristóbal, F. Truchetet, and P. Saarikko, eds., Proc. SPIE **7723**, 77230X (2010).
26. C. Hoepfner, "PhlatLight photonic lattice LEDs for RPTV light engines," *SID Symposium Digest* **37**, 1808–1811 (2006).

---

## 1. Introduction

Multiview displays show many view images of an object to perceive depth [1]. Unlike stereoscopic displays [2] they do not require special eyeglasses. This is made possible by generating many viewing zones: a region in which only one view image is visible. These viewing zones are sufficiently narrow in order that the left and right eye see a different image. The parallax between both images is used to perceive depth. In addition, motion parallax depth cues are available. When the viewer moves from left to right, the eyes will pass adjacent viewing zones and see the object from a different direction. This is often referred to as look-around capability and can be experienced by multiple viewers at the same time. Multiview displays have the potential to be as realistic as holograms. For this, the viewing zones have to be extremely narrow in order that more than one view image is incident on each eye pupil [3, 4, 5]. This solves the accommodation-vergence conflict that causes visual discomfort in many stereoscopic and autostereoscopic systems. This type of multiview displays is often called super multiview.

The view images can either be simultaneously or time-sequentially generated by a flat panel display, one or many projectors or a combination of both. Firstly, a lenticular sheet or parallax barrier can be added to a flat panel display [6, 7, 8]. This approach provides a compact solution using widespread technology but with limited performance. The view images are spatially multiplexed over the display surface and shown at the same time. Because of this, the spatial resolution of the object will decrease when the number of viewing zones is increased.

By slanting the viewing optics, the resolution loss is divided over the horizontal and vertical directions. So, a full HD panel (1920x1080 pixels) will enable a 9-view system with a spatial resolution of 640x360 pixels. Other issues are the reduced image brightness of parallax systems, the occurrence of many copies of the view images, crosstalk between viewing zones and the non-uniform angular distribution of the viewing zones. In 2009 Takaki [9] proposed and demonstrated a slanted sub-pixel arrangement instead of a slanted lenticular sheet that has a uniform angular distribution without crosstalk. Secondly, projectors can be used to create multiview displays. One single projector with a configurable slit aperture in the projection lens [10] or a directional illumination of the light modulator [11] can realize this. All view images are time-sequentially modulated by the same device. Therefore, a high-speed projector is necessary. Kanebako [11] reported a digital light processing (DLP) projection system with directional illumination of the micromirrors by 15 monochrome light emitting diodes (LEDs). This approach can be interpreted as image steering at the light modulator level. DLP technology is considered because of its high-frame-rate capability [12]. 50 Hz monochrome operation with 15 viewing zones was achieved in 5-bit gray scale. To show full-color images, the number of viewing zones or the number of gray scales have to decrease. The main advantage of these single-projector systems is that the spatial resolution of the view images is the same as that of the light modulator irrespective of the number of viewing zones and that the system can be potentially low cost. On the other hand, the brightness of the images decreases when the number of viewing zones is increased because the useful étendue of each view image is limited to the total system étendue divided by the number of viewing zones. Multiview projection systems also exist that use the same number of projectors [13] or light modulators [5] than viewing zones. This has the advantage that the light modulators do not have to operate time-sequentially and so high-resolution low-speed light modulators can be considered. Takaki [5] reported a 64-view system using 64 transparent color liquid crystal light modulators. Kikuta [14] reported a 128-view system using 128 reflective liquid crystal light modulators. Such systems are large, complex and expensive, but the high number of viewing zones can enable super multiview operation. A final approach combines the spatial multiplexing of flat panel displays with multiple projection systems. Takaki [15] reported a system using 16 liquid crystal displays with each 16 viewing zones enabled by a lenticular sheet. All images are combined to form a 256-view system with a lower cost than a 256-projector system, but with reduced spatial resolution.

When designing a multiview display one has to take into consideration the desired spatial and angular resolution, brightness, system dimensions, operational speed and cost. We want to develop a multiview system with high spatial resolution. Therefore, we consider a projection approach. Additionally, the system should be potentially low cost and compact. For this reason, we use only one projector that time-sequentially modulates the view images. We also want to show high-brightness images with high-angular resolution. This requirement is not compatible with the discussed state-of-the-art single-projector systems because the brightness of the view images decreases with the number of viewing zones. We have developed an image steering projection screen that time-sequentially steers images into different viewing zones. Each image is created using the entire system étendue of the projector. In this way, the image brightness does not decrease with the number of viewing zones. The screen is based on the concept of beam steering using decentered microlens arrays [16]. This concept has strictly been applied for the steering of coherent light in telescopes [17], infrared countermeasures, optical switches and laser radar.

In this paper, we will discuss a prototype multiview display using a single projector and an image steering projection screen. Moving microlens arrays have already been reported in 3D displays [18]. To our knowledge, this is the first time that decentered microlens arrays are implemented in the projection screen of such systems. In Sec. 2 we overview the working

principle of our multiview display. In Sec. 3 we discuss the design and implementation of the projector and the image steering projection screen. In Sec. 4 we calculate the number of viewing zones the system can show and experimentally characterize the prototype system. Finally, we discuss system modification and enhancements in Sec. 5 and conclude in Sec. 6.

## 2. Image steering projection screen

### 2.1. Beam steering

The multiview display is based on time-sequentially projecting the view images onto a screen that steers each image into a different direction. This concept is illustrated in Fig. 1. The projector is located behind the projection screen because the image steering results from refraction of light propagating through a microlens system implemented in the screen. This microlens system consists of three microlens arrays as is shown in Fig. 2. To explain its operating principle, let us consider one beam steering element which consists of three microlenses one after the other. The light is steered in different directions by equally changing the decenter  $\delta$  between the first lens and the second lens, and the first lens and the third lens. The second lens is placed at the back focal plane of the first lens and at the front focal plane of the third lens. Ideally, the first lens focuses a collimated light beam to a point at the second lens which is again transformed to a collimated light beam by the third lens. If the second and third lens are decentered with respect to the first lens, the focused light point at the second lens will appear as an off-axis point for the third lens, and the direction of the collimated light beam will change. The second lens is necessary to ensure a high fill factor of the third lens at large steering angles and to avoid crosstalk between adjacent beam steering elements which leads to undesired beam directions

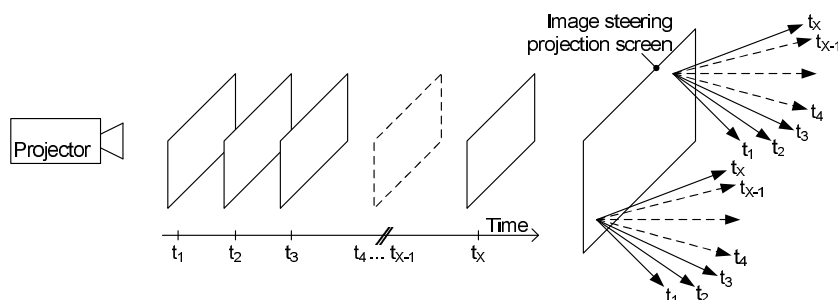


Fig. 1. Schematic illustration of the time-sequential operation of the multiview display.

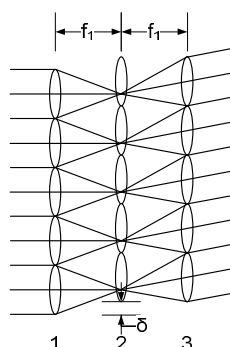


Fig. 2. Beam steering using decentered microlens arrays.

[16]. We consider that the second lens has the same optical properties as the third lens.

## 2.2. Screen dimensions

The microlens arrays cover the entire screen surface in order to steer the entire image. In total, there are as many beam steering elements on the screen as pixels in the image. Each beam steering element changes the propagation direction of one pixel. We consider a projector with DLP technology [12]. This choice is based on the high-frame-rate capability of DLP projection systems which is crucial for time-sequential multiview systems [11]. For example, 20 viewing zones and a refresh rate of 50 frames per second necessitate a frame rate of 1000 images per second. Furthermore, we consider a projection architecture with only one digital micromirror device (DMD) light modulator to limit the cost of the multiview display. This implies that the spatial light modulator has to color-sequentially modulate the images. Such high frame rates are not possible with transmissive or reflective liquid-crystal-based spatial light modulators [19, 20]. DLP projection systems rely on electrostatic actuation of micromirrors by voltage differences between the mirror and the underlying memory cell. Each pixel on the screen is modulated by a single square-shaped micromirror. It can switch between two orientation states by tilting  $12^\circ$  about hidden diagonal hinges. The switching time is about  $5.5 \mu\text{s}$  (DMD Discovery 3000). Another  $8 \mu\text{s}$  are needed for the micromirror to reach a stable state. When a micromirror is in the on state, light will be reflected to the projection lens and a bright pixel is seen on the projection screen. When a micromirror is in the off state, light will be reflected to a light absorber and the pixel is dark. By varying the on and off time, during each image frame, gray levels are obtained.

We use a DMD light modulator with XGA resolution ( $1024 \times 768$  pixels). The projection setup is shown in Fig. 3. The micromirrors have a pitch of  $13.68 \mu\text{m}$  and a fill factor of 85%. They are imaged by the projection lens and form pixels with a pitch of  $500 \mu\text{m}$  on the projection screen. The width of the image is  $51.2 \text{ cm}$  and the height is  $38.4 \text{ cm}$ . Consequently, the microlens arrays have to cover a surface with a  $25 \text{ in.}$  diagonal ( $1 \text{ in.} = 2.54 \text{ cm}$ ).

## 2.3. Microlens specifications

We have designed the microlenses to enable horizontal parallax images. For this, we use vertically-oriented cylindrical microlenses in combination with horizontal decenter. The microlenses have a footprint of  $500 \mu\text{m}$  which is equal to the pixel pitch. We consider a maximal decenter of  $225 \mu\text{m}$  to steer the light (90% of half the footprint of the microlenses). We work

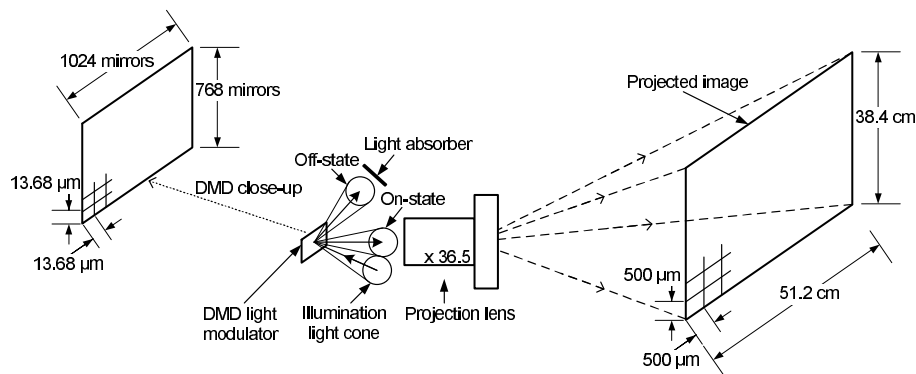


Fig. 3. Schematic illustration of the projection setup using a DLP projector with a single DMD light modulator.

with two lens sheets: one which contains the first microlens array and one which contains both the second and the third microlens array on opposite sides of the lens sheet. The lens sheets are made out of glass with polymer microlenses on its surface [21]. In front of the first lens sheet, we place a large Fresnel lens to collimate the light rays of the projected image. Behind the second lens sheet, we place a diffuser to spread the steered light beam in the vertical direction.

The microlenses are optimized to obtain a broad steering range and minimal divergence of the steered light beam. The latter is essential to achieve many viewing zones. For this, we used the nonsequential ray-tracing program ASAP from Breault Research Organization. The input light distribution of each microlens on the first lens sheet has a square-shaped spatial distribution of  $461 \mu\text{m} \times 461 \mu\text{m}$  and a cone-shaped angular distribution with a half-angle of  $0.328^\circ$ . The latter corresponds to the illumination light cone of the DMD light modulator divided by the magnification of the projection lens (étendue conservation). In Fig. 4, we show the optimized design of the lens sheets. Both lens sheets are separated by a distance equal to 1 mm. The first lens sheet is  $400 \mu\text{m}$  thick and the second lens sheet  $1200 \mu\text{m}$ . Their thickness is sufficient to provide stability for the considered screen size. When the decenter is zero, the light beam propagates straight on. When the decenter is maximal ( $225 \mu\text{m}$ ), the light beam is steered  $15.4^\circ$ . For negative decenter values, the magnitude of the steering angle is the same as for positive decenter values, but the direction is opposite.

The numerical values of the steering angle and the divergence of the outgoing light beam for different horizontal decenter values are shown in Fig. 5. We see that the steering angle linearly increases as a function of the decenter and that the beam divergence slightly increases for larger steering angles. The latter is caused by system aberrations when the focused light spot at the second lens moves away from the optical axis of the second and third lens for larger decenter values. On average, the full-angle divergence of the light beam is  $1^\circ$ .

### 3. System architecture

#### 3.1. DLP projector with LED light sources

The projector, using only one DMD light modulator, has to time-sequentially modulate the three color components of all view images. For this, the DMD light modulator is consecutively illuminated by red, green and blue (RGB) light. Due to the required high frame rate of the

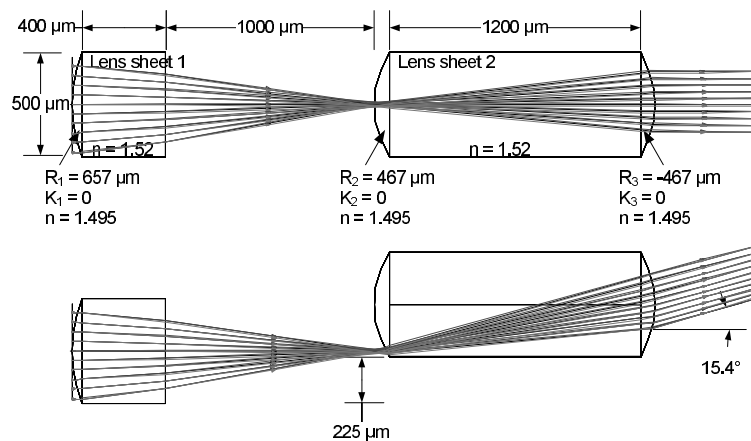


Fig. 4. Horizontal cross section of one beam steering element on both lens sheets. One pixel of the image is traced through the lens system with no decenter (top) and with maximal decenter (bottom).

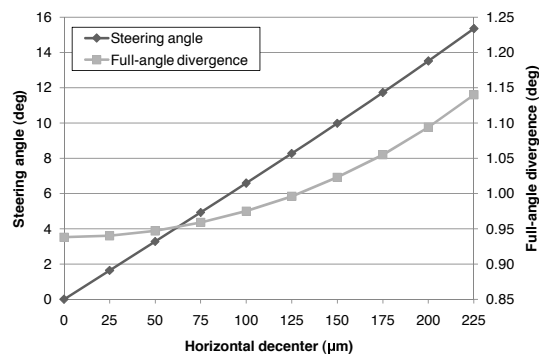


Fig. 5. The simulated steering angle and full-angle divergence of the steered light beam throughout the decenter range.

projector, we decided to use high-power LEDs as projection light sources because they can be rapidly switched on and off, and because they are available in the primary colors of the display [22, 23, 24].

We have reengineered the optical module of a 0.7 in. XGA DMD Discovery 3000 development kit, for RGB LED illumination [25]. We designed a compact illumination system that collects and combines the light of one red, green and blue PT54 PhlatLight LED [26]. This light output is made uniform by a rod integrator and then imaged onto the DMD light modulator. The projector has a light output of 80 ANSI lumen and a contrast ratio of 680:1. The LEDs have an average power consumption of 20 W.

### 3.2. Vibrating projection screen

We want to operate the multiview system at a refresh rate of 50 Hz to avoid flickering images. This implicates that 50 images are directed into each viewing zone per second. For this, the second lens sheet is moved from the outmost right position (225 μm) to the outmost left position (-225 μm) while the view images are time-sequentially projected and steered into the respective viewing zone. Next, the second lens sheet is moved back to its starting position and the view images are shown in opposite order. This process is repeated 25 times per second to achieve a 50 Hz refresh rate.

The mechanism that moves the second lens sheet, back and forth, has to operate at a frequency of 25 Hz and a travel range of 450 μm. Furthermore, it has to be sufficiently powerful (push-pull force) and it has to move with high accuracy and repeatability. The 1.2 mm thick glass lens sheet weighs 730 g and it is held in an aluminum frame that weighs 350 g. Additionally, the vertical diffuser is attached to the moving lens sheet which increases the weight with 215 g. We considered using a linear translation stage with a servo motor, but the required mechanical transmission to enable the push-pull force did not allow 25 Hz operation. This is also valid for piezoelectric actuators. Furthermore, the relative large travel range would require a very long piezoelectric stack. We solved the force-frequency issue by implementing the screen motion as a mass-spring system that oscillates at its natural frequency. In this way, a low-power motor can be used because the motion is self-sustaining.

To create the mass-spring system, leaf springs are attached on both sides of the aluminum frame and connected to a fixed structure which is also used to position the first lens sheet. This is shown in Fig. 6. The spring constant of these leaf springs is chosen in order that the natural frequency of the screen equals the desired oscillation frequency of 25 Hz. We use a DC-motor that operates at 1500 rpm. It has a magnetic encoder to determine the screen position during the

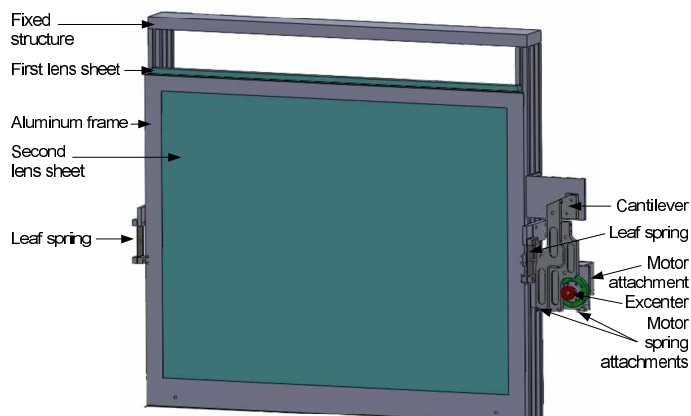


Fig. 6. CAD drawing of the moving mechanism. The moving lens sheet is part of a mass-spring system.

motion. An excenter is connected to the motor shaft which initiates the oscillating motion. The excenter is in contact with a cantilever which has a fixed connection to the aluminum frame of the second lens sheet. During half the rotation of the motor shaft, the excenter pushes the screen away ( $225 \text{ m}$  to  $-225 \text{ m}$  decenter). During the other half of the rotation, a set of two springs in the motor setup ensures that the excenter remains in contact with the cantilever while the screen returns to its start position ( $-225 \text{ m}$  to  $225 \text{ m}$  decenter). In this way, the amplitude of the oscillation is perfectly  $450 \text{ m}$ . When the motor is powered off, the motor springs ensure that the screen stops at the start position. The screen motion is sinusoidal with both a horizontal and vertical component. The horizontal component is the desired decenter between both lens sheets that controls the beam steering direction. The vertical component does not impact the beam steering because the lens sheets consist of vertically-oriented cylindrical microlenses.

The screen structure has several alignment features to position both lens sheets with respect to each other. Firstly, it is possible to change the orientation of the second lens sheet in order that the cylindrical lenses are parallel to those on the first lens sheet. Secondly, the distance between both lens sheets can be adjusted. Finally, the horizontal starting position and the amplitude of the motion can be fine-tuned.

#### 4. Implementation of a 27-view system

##### 4.1. Number of viewing zones

The image steering projection screen moves continuously back and forth while images are color-sequentially and view-sequentially projected onto it. Because the red, green and blue color components of each view image are not shown at the same time, their steering direction will be different. This has to be kept minimal in order to perceive the three colored light beams as one light beam with the correct color information; the steering range of each viewing zone has to be about the same size as the divergence of the steered light beam. If the steering range is much larger, the viewing zone will be split into three separate parts with different colors and the eye will not see the correct color information.

We used the ALP-3 high speed controller board to access the DMD light modulator. The number of image frames it supports per second is given in Table 1. We see that in 8-bit gray scale a total of 250 image frames can be modulated per second. Three image frames are needed to modulate one full-color image. To show one viewing zone, a total of 150 image frames are



Table 1. Overview of the number of image frames the DMD can modulate and the number of viewing zones this corresponds to.

Gray scale (bit)	Max. switching rate (frames/sec)	Number of viewing zones
1	13333	88
2	5319	35
3	3546	23
4	2315	15
5	1462	9
6	864	5
7	476	3
8	250	1

needed. This corresponds to the refresh rate of 50 Hz and full-color operation. Because of this, the DMD projector can only show one viewing zone with 8-bit images. By decreasing the bit depth, the modulation time becomes smaller and the number of image frames increases. 5-bit images already enable 9 viewing zones, but within a steering range of approximately  $30^\circ$  and a full-angle divergence of  $1^\circ$  this is not sufficient to obtain a uniform angular distribution. Therefore, we further decreased the bit depth to 2-bit which enables a maximal number of 35 viewing zones.

The sinusoidal motion of the screen has to be taken into account to determine the number of viewing zones. In Fig. 7, we show the calculated angular distribution of 35 images modulated in a time period of 20 ms (50 Hz, 225  $\mu$ m to -225  $\mu$ m decenter). We see that the steering angle changes sinusoidally. This is because the change in decenter, during the fixed time period to modulate each 2-bit full-color image, is not constant, but sinusoidal. In the beginning of the motion (225  $\mu$ m decenter), the velocity of the screen is minimal resulting in a small steering range ( $0.06^\circ$ ). The steering range then gradually increases while the velocity of the screen increases until halfway the motion (0  $\mu$ m decenter) where the steering range is maximal ( $1.36^\circ$ ). Next, the steering range decreases until the end of the motion (-225  $\mu$ m decenter). This process is repeated while the screen returns to its start position. Thus, the steering range of the images with large steering angles (begin and end) is smaller than the images with small steering angles (middle). For images 1 to 4 and 32 to 35, the steering range is less than half the divergence of the steered light beam. These images will largely overlap and the image information will be distorted by crosstalk. This can be solved by repeating the image information during consecutive images and thereby combining several images into one viewing zone with sufficient steering range. We will show the same image information during images 1 to 4, 5 and 6, 30 and 31 and, 32 to 35. In this way, we obtain 27 viewing zones with a minimal steering range of  $0.75^\circ$  and a maximal steering range of  $1.36^\circ$ . On average, the steering range is  $1.12^\circ$  which is slightly more than the beam divergence.

#### 4.2. Synchronization and timing

The screen has to be perfectly synchronized with the projector to steer the image information into the correct direction. For this, we have implemented a synchronization module based on a field-programmable gate array (FPGA) that instructs the projector to show two sets of view images each time the screen is in its start position (25 Hz). Each set consists of 35 2-bit full-color images (105 image frames). The first set of images is time-sequentially directed into

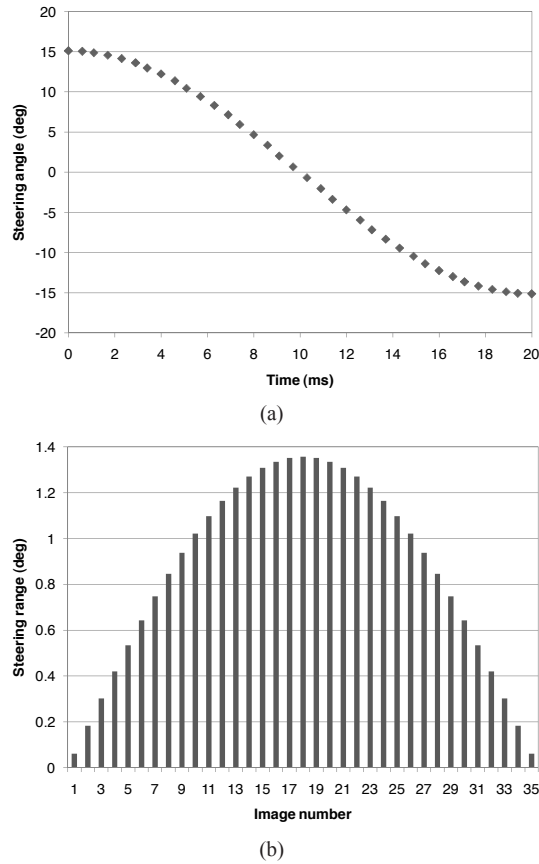


Fig. 7. Calculated angular distribution of 35 2-bit full-color images. The steering angle (a) and steering range (b) of each image during the sinusoidal motion of the screen.

viewing zone 1 to 27 (225 m to -225 m decenter), the second set of images into viewing zone 27 to 1 (-225 m to 225 m decenter).

Every 190 μs an image frame is modulated. For this, the FPGA triggers the DMD to show the next image frame and turns on the LED with the color of the image information. The DMD is configured to modulate the image frame in 189 μs. During the first 114 μs, the two bit planes of the image frame are modulated. The remaining 75 μs is used to upload the first bit plane of the next image frame in the memory cells beneath the micromirrors. The LED illuminates the DMD during the first 114 μs. We remark that the 1 μs difference between the image frame time and the image modulation time is used by the DMD controller board to detect the next rising edge of the trigger signal. The prototype system is shown in Fig. 8

#### 4.3. Experimental characterization

We have demonstrated the multiview projection display for still images. We created a 27-view image set of a virtual object taken from different camera positions that correspond with the direction of the viewing zones. The viewer perceives a 3D image without special eyeglasses from a viewing distance between 1 m and 4 m with look-around capability. For smaller viewing distances, the entire image is not visible because of the limited steering range. For larger viewing distances, only two-dimensional images are seen because the viewing zones are expanded to



Fig. 8. Picture of the prototype system. The projector is located on the left and the image steering projection screen on the right. The 3D images are seen on the other side of the projection screen (Media 1).

the extent that both eyes see the same image.

To characterize the operation of the entire system, we measured the angular distribution of the viewing zones. For this, we projected a black image with a white spot in the middle, and investigated the position of the steered light spot at a viewing distance of 1 m. The spot is only a few pixels wide in order not to contribute to the width of the viewing zones at the detection plane. In Fig. 9, we show a picture of the steered light spot using an image set that consists of the black image with the white spot in all odd viewing-zone positions and a plain black image in all even viewing-zone positions. The picture is taken with a shutter speed of 1 s and therefore consists of 50 traces of the image steering. Each light spot corresponds to one viewing zone with odd numbering. It can be interpreted as the print of all directions in which light is steered during the time that the red, green and blue color components of that viewing zone are modulated. The angular distribution of the viewing zones is shown in Fig. 10. Both subfigure are based on a different image set; in Fig. 10(a) we examine the odd and even viewing zones separately and in Fig. 10(b) we use the black image with the white spot for all viewing zones to examine the uniformity of the steered light throughout the steering range. We find that the intensity of the first and last viewing zone, and the second and second last viewing zone are respectively four and two times larger than the other viewing zones. This can be explained by the fact that in these viewing zones, respectively, four and two images are used to form the viewing zone (Section 4.1). Therefore, the intensity is higher than in the other viewing zones that appear by steering one image only. The global U-shaped angular intensity distribution also shows spikes of about 10%. These correspond to the angular intensity distributions of the viewing zones that do not form a flat intensity distribution when summed. To achieve this, the angular intensity distribution of each viewing zone should be a flat-to distribution. We also find that the steering range corresponds to the simulated range of the lens sheets (Section 2.3) and that the color components of each viewing zone do not perfectly overlap: red is visible on the left and blue on

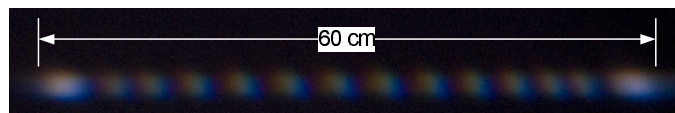


Fig. 9. Picture of the odd viewing zones at a viewing distance of 1 m (from left to right, numbers: 1, 3, 5, 7, 9, 11, 13, 15, 17, 19, 21, 23, 25 and 27).

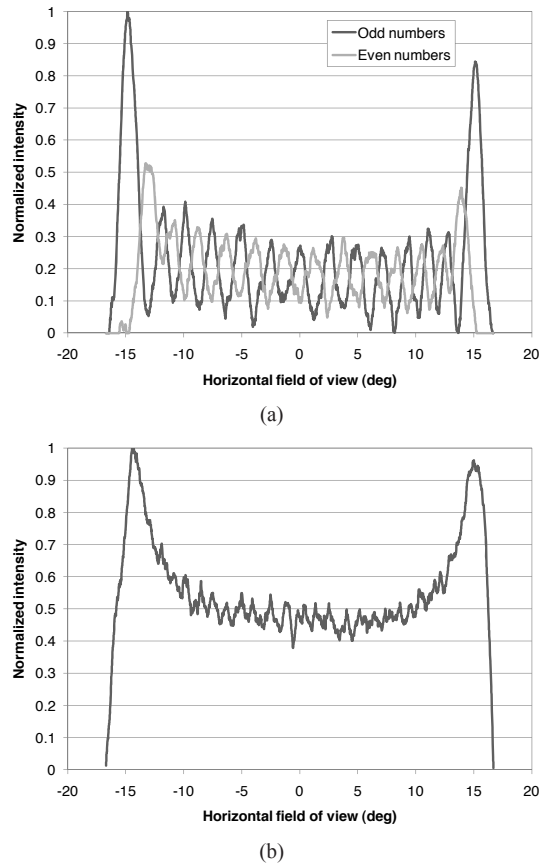


Fig. 10. Measured angular distribution of the viewing zones (a) and the uniformity of the steered light (b).

the right. Because of the overlap of adjacent viewing zones, we still perceive the correct color information.

#### 4.4. Image artifacts

Every view image is repeated 50 times per second, yet the viewer does not perceive flicker-free images from all viewing positions. We find that in the center of the viewing space the refresh rate is 50 Hz whereas toward the sides the refresh rate decreases to 25 Hz. This can be explained by considering the time between two images that are directed by the screen into the same viewing zone. This is shown in Fig. 11. Because both directions of the sinusoidal-screen motion are used to show images, the time between two consecutive images is not the same for all viewing zones. For the outmost viewing zones (1 and 27), the images follow immediately one after the other. The eye integrates these images and only sees one image each 40 ms. Therefore, the refresh rate is perceived to be 25 Hz instead of 50 Hz. On the other hand, in the center (viewing zone 14), the time between two consecutive images is exactly 20 ms and the refresh rate is perceived correctly (50 Hz).

The images that are visible on the vibrating screen are distorted by Moiré patterns as is visible in Fig. 12. These image artifacts result from the optical sampling of the images, projected onto the screen, by the periodic elements in the screen. These are the Fresnel lens, the vertically-

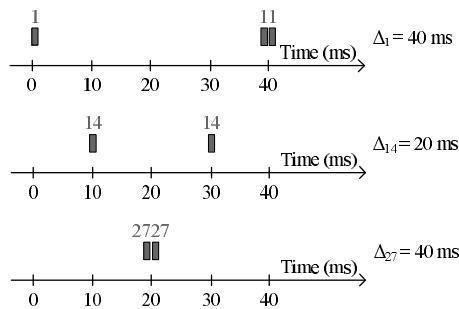


Fig. 11. The time between consecutive images in viewing zones 1, 14 and 27 (225 mm, 0 mm and -225 mm decenter, respectively).

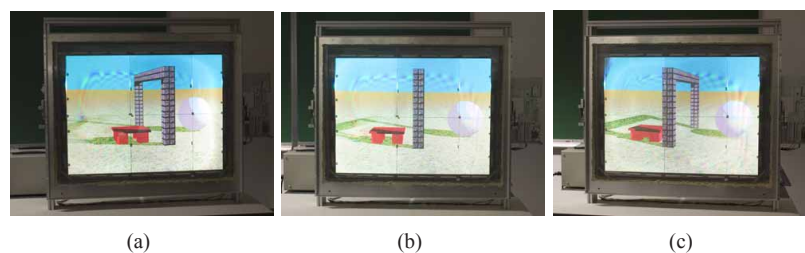


Fig. 12. Picture of the Moiré patterns on the vibrating screen. Outmost left viewing zone (a), center viewing zone (b) and outmost right viewing zone (c).

oriented cylindrical microlenses and the holographic vertical diffuser. They can cause radial, horizontal and vertical sampling, respectively. The pitch of the Fresnel lens structures is about five times smaller than the pixel pitch. Therefore, the radial sampling frequency is high enough to avoid aliasing. On the other hand, the pitch of the cylindrical lenses is designed to be the same as the pixel pitch. Small variations of the lens pitch and the pixel pitch introduce Moiré patterns. The pitch of the holographic diffuser is much smaller than the pixel pitch and does not contribute to the Moiré patterns.

## 5. Discussion

We have demonstrated a multiview display capable of showing horizontal parallax images by means of image steering. To progress toward higher angular resolution or larger field of view or horizontal and vertical parallax images combined, even more images will have to be modulated. This requires modification and enhancements of the DMD projector as well as the image steering projection screen.

Showing more images is limited with the current DMD projector because it would imply a further decrease of the bit depth of the images from 2 bit to 1 bit. A possible solution is to use three DMD light modulators instead of only one. The color components of the view images can then be shown at the same time instead of color sequentially. This has the advantage that each DMD light modulator has to modulate three times less images compared to a single DMD light modulator approach and that the color components of each viewing zone will perfectly overlap. In our demonstrator system, this approach would enable 4-bit images, an improvement of the number of gray scales with a factor four. Also, the brightness of the images would increase. Nevertheless, the increase of the number of images is not sufficient to allow systems with the envisioned multiview characteristics. This will also require a significant increase of the

performance of the DMD controller board, the DMD driver electronics and the DMD chip itself. Furthermore, innovative modulation techniques can be used to maximize the frame rate. For example, by intensity modulation of the LED illumination in order to show the same bit depth in a shorter time. Other spatial light modulators such as liquid-crystal-on-silicon devices cannot currently be considered because they are not fast enough. On the other hand, in most cases, they do have the benefit of being an analog technology and thereby providing full bit depth.

Higher angular resolution will require the viewing zones to be narrower. For this, it will be necessary to decrease the divergence of the steered light beam. This is possible when the étendue of the light processed by each microlens decreases. A DMD projector based on laser illumination could be appropriate for this. A larger field of view will require microlenses with a smaller f-number and additional vertical parallax will necessitate microlenses with a square footprint and also vertical screen motion.

The optical and mechanical implementation of the image steering projection screen can be improved in several ways. We experienced that it is difficult to set the distance between the lens sheets to 1 mm over the entire screen surface. Deviations result in larger beam divergence and consequently the view images overlap. This can be improved by increasing the necessary distance between both lens sheets in order to make the relative errors smaller. Also, we experienced that the lens sheets are fragile and that they can slightly be bent. This can be improved by making them thicker. The Moiré patterns can be eliminated by making the pitch of the microlenses at least two times smaller than the pixel pitch. Furthermore, antireflection coatings will improve the transmission efficiency of the rear-projection screen; currently, the transmission is 66% (Fresnel lens 92%, lens sheet 1 92%, lens sheet 2 92% and diffuser 85%). The mechanical part of the screen can be improved by adding a feedback control system to compensate for frequency fluctuation of the motor. Also, the oscillation frequency has to be increased in order to obtain flicker-free images for the entire field of view. A first approach is to double the oscillation frequency of the screen (25 Hz to 50 Hz) and to show images only in one direction of the motion (225  $\mu$ m to -225  $\mu$ m decenter). This has the advantage that the refresh rate of all view images will be equal to 50 Hz, but the disadvantage that the brightness of the system will decrease with 50% because only half of the screen motion is used to show the images. Another approach is to continue showing the images during both directions of the motion. Because of this, the refresh rate will not be the same for all viewing zones, but it will be high enough to ensure flicker-free operation for the entire field of view (outmost viewing zones 50 Hz and center viewing zone 100 Hz). We remark that both approaches, again, increase the number of images that have to be shown. The angular spread of the viewing zones can be decreased by implementing a stepwise motion instead of a continuous motion. The screen moves to its new position and then images are projected onto it. Because of this, the angular spread of each viewing zone will be equal to the divergence of the steered light beam. Also, the color components of each viewing zone will perfectly overlap. Finally, the entire system can be made more compact by folding the optical path from the projector to the screen.

## 6. Conclusion

We have implemented the concept of beam steering using decentered microlens arrays for multiview displays. We designed and demonstrated a rear-projection system using a single projector and an image steering projection screen. The latter consists of two lens sheets covered with vertically-oriented cylindrical microlenses. The horizontal decenter between the microlenses on both lens sheets determines the horizontal steering direction. The view images of a 3D object are time-sequentially projected onto the screen and steered into the respective viewing zone by changing the relative position of the lens sheets.

The screen has a diagonal of 25 in. and contains microlenses with a footprint of 500  $\mu\text{m}$  which corresponds to the pitch of the pixels in the images that are projected onto it. The decenter between the microlenses ranges between 225  $\mu\text{m}$  and -225  $\mu\text{m}$ . This enables beam steering from  $15^\circ$  to  $-15^\circ$  with a full-angle beam divergence of  $1^\circ$ . The projector shows all view images in full-color at a refresh rate of 50 Hz. To accomplish this, we have designed a DLP projector with LED light sources. The moving lens sheet in the projection screen is implemented as a mass-spring system that oscillates at 25 Hz. The resulting prototype shows a total of 27 viewing zones with XGA resolution within a horizontal field of view of  $30^\circ$ . The bit depth of the images is reduced to 2 bit. This is required to modulate the high number of image frames.

The demonstrated system can show high-brightness multiview images with high-angular resolution using a single projector. The spatial resolution of the images is determined by the projector. The system has the potential to progress toward super multiview with both horizontal and vertical parallax by significantly increasing the frame-rate capability of the DLP projector and by adapting the projection screen to steer narrower beams of light.

### **Acknowledgments**

This work is supported by the Research Foundation - Flanders (FWO-Vlaanderen). We also acknowledge the Industrial Research Funding (IOF), the Methusalem and Hercules foundations, VUB-GOA, and the OZR of the Vrije Universiteit Brussel. Lawrence Bogaert is indebted to FWO-Vlaanderen for an Aspirant grant.